The American Journal of Pathology, Vol. 179, No. 3, September 2011

DOI: 10.1016/j.ajpath.2011.05.055

Musculoskeletal Pathology

Inclusion Body Myositis

Laser Microdissection Reveals Differential Up-Regulation of IFN-γ Signaling Cascade in Attacked versus Nonattacked Myofibers

Jana Ivanidze,*† Reinhard Hoffmann,‡ Hanns Lochmüller,§ Andrew G. Engel,¶ Reinhard Hohlfeld,*† and Klaus Dornmair*†

From the Institute of Clinical Neuroimmunology, Ludwig Maximilians University, Munich, Germany; the Department of Neuroimmunology,† Max-Planck-Institute of Neurobiology, Martinsried, Germany; the Institute for Medical Microbiology, Immunology and Hygiene,‡ Technische Universitaet Munich, Munich, Germany; The Institute of Human Genetics,§ Newcastle University, International Centre for Life, Newcastle upon Tyne, United Kingdom; and the Neuromuscular Research Laboratory,¶ Mayo Clinic and Foundation, Rochester, Minnesota*

Sporadic inclusion body myositis (IBM) is a muscle disease with two separate pathogenic components, degeneration and inflammation. Typically, nonnecrotic myofibers are focally surrounded and invaded by $CD8^+$ T cells and macrophages. Both attacked and nonattacked myofibers express high levels of human leukocyte antigen class I (HLA-I) molecules, a prerequisite for antigen presentation to $CD8^+$ T cells. However, only a subgroup of HLA-I^+ myofibers is attacked by immune cells. By using IHC, we classified myofibers from five patients with sporadic IBM as attacked (A_{IBM}) or nonattacked (N_{IBM}) and isolated the intracellular contents of myofibers separately by laser microdissection. For comparison, we isolated myofibers from control persons (H_{CTRL}). The samples were analyzed by microarray hybridization and quantitative PCR. HLA-I up-regulation was observed in A_{IBM} and N_{IBM}, whereas H_{CTRL} were negative for HLA-I. In contrast, the inducible chain of the interferon (IFN) γ receptor (IFNGR2) and several IFN-γ–induced genes were up-regulated in A_{IBM} compared with N_{IBM} and H_{CTRL} fibers. Confocal microscopy confirmed segmental IFNGR2 up-regulation on the membranes of A_{IBM}, which positively correlated with the number of adjacent $CD8^+$ T cells. Thus, the differential up-regulation of the IFN-γ signaling cascade observed in the attacked fibers is related to local inflammation, whereas the ubiquitous HLA-I expression on IBM muscle fibers does not require IFNGR expression. ***(Am J Pathol 2011, 179:1347–1359; DOI: 10.1016/j.ajpath.2011.05.055)***

Sporadic inclusion body myositis (sIBM) is the most common inflammatory myopathy in adults >50 years presenting with progressive weakness and atrophy of both proximal and distal muscle groups and leading to disability within 5 to 10 years after diagnosis.[1,2] Because sIBM, in contrast to polymyositis (PM) or dermatomyositis (DM), is notoriously refractive to immunosuppressive therapies,[3,4] it is assumed that sIBM is not a primary autoimmune myopathy but that the inflammatory changes are secondary to as yet unknown viral or degenerative triggers.[5] Therefore, sIBM is regarded as the paradigm of a myopathy with distinct degenerative and inflammatory pathogenetic components.[1,6]

The mechanism of inflammatory myofiber injury is unique in that $CD8^+$ T cells and macrophages focally surround and invade initially nonnecrotic myofibers.[7] Several articles[6,8,9] provide a review of this information. The myoinvasive $CD8^+$ cytotoxic T cells likely recognize (still unknown) antigens presented by HLA class I (HLA-I) molecules on the myofiber surface.[10] Antigen-driven recruitment of the myocytotoxic $CD8^+$ T cells is supported by evidence that the T cells are clonally expanded, using a restricted repertoire of T-cell

Supported by a scholarship from the Gerhard C. Starck Foundation, Düsseldorf, Germany (J.I.). H.L. is an investigator at the MRC Centre for Neuromuscular Diseases and at TREAT-NMD (EC, 6th FP, proposal 036825).

Accepted for publication May 31, 2011.

R.Hoh. and K.D. contributed equally to this work.

Supplemental material for this article can be found at *http://ajp.amjpathol.org* or at doi:10.1016/j.ajpath.2011.05.055.

Address reprint requests to Reinhard Hohlfeld, M.D., or Klaus Dornmair, Ph.D., Institute of Clinical Neuroimmunology, Ludwig Maximilians University, D-81377 Munich, Germany. E-mail: reinhard.hohlfeld@med.uni-muenchen.de or dornmair@neuro.mpg.de.

Table 1. Overview of the Basic Characteristics of Patients and Healthy Controls

Patient or control	Diagnosis	Age (years)	Sex	Biopsied muscle	No. of isolated myofibers to reach >100,000 μm^{2*}
Patient no.					
IBM-1	sIBM	75	Male	Biceps brachii	43/37
IBM-2	sIBM	70	Male	Vastus lateralis	42/35
IBM-3	sIBM	79	Female	Biceps brachii	42/38
IBM-4	sIBM	69	Male	Triceps brachii	50/41
IBM-5	sIBM	72	Male	Triceps brachii	50/47
Control no.					
C-1	Nonspecific myalgia, depression	57	Male	Biceps brachii	55
C-2	Nonspecific myalgia	61	Male	Biceps brachii	60
C-3	Nonspecific myalgia	52	Male	Rectus femoris	57

Five patients with sIBM and three controls were included in the study. Their clinical and histopathological characteristics are listed. The congophilic deposits were visualized in Congo red–stained sections viewed under rhodamine optics. All biopsy specimens of patients with sIBM showed rimmed vacuoles, autoaggressive inflammatory exudates, and congophilic inclusions. IBM-2 presented additional mitochondrial dysfunction. IBM-4 and IBM-5 additionally displayed atrophic myofibers. C-1 had a clinically silent leukocytosis with C-reactive protein elevation at biopsy. C-2 showed no abnormalities on muscle biopsy or laboratory results. C-3 presented with status post statin therapy with transient slight creatine kinase elevation; however, the muscle histology was negative and there were no other abnormalities. The biopsied muscle is included, along with the number of laser-microdissected myofibers that, in each case, compose a total of 100,000 μm^2 of myofiber area. The number of myofibers varies in the patients with sIBM given the high variability in myofiber diameter. Control fibers, in general, were smaller on average and, thus, more fibers had to be sampled from controls.

*For patients, data are given as A_{IBM}/N_{IBM}.

receptors[11–15] and persisting over time in individual patients.[12,15,16] Moreover, the $CD8^+$ T cells form specific immunological synapses with vectorial excretion of perforin toward the attacked myofibers.[17] This cytotoxicity cannot be assessed in *in vitro* co-culturing experiments because only alloreactive $CD8^+$ T cells were strongly cytotoxic to allogenic myotubes in co-cultures.[18,19]

HLA-I is not detectable on myofibers of healthy subjects.[20] In sIBM, HLA-I is uniformly up-regulated on all myofibers[21–24]; however, $CD8^+$ T cells attack myofibers in a strictly focal pattern.[25] Obviously, HLA-I expression is only a necessary, but not sufficient, precondition for a myofiber to be attacked. There seem to be additional factors rendering muscle fibers susceptible to inflammatory attack. The aim of the present study was to identify molecular patterns that are differentially regulated in invaded versus noninvaded muscle fibers, focusing on the pathways of antigen presentation and processing.

To address the question of why certain myofibers are attacked, whereas others are spared, we used the unique properties of the distinct morphological characteristics of myofibers that remain clearly distinguishable, even under conditions required for laser microdissection (ie, nonembedded tissue and short incubation times, as described in *Materials and Methods*). We separately laser microdissected attacked and nonattacked muscle fibers while excluding inflammatory cells. We compared attacked myofibers from IBM muscle (A_{IBM}), nonattacked sIBM myofibers (N_{IBM}), and healthy control myofibers (H_{CTRL}) using microarray transcriptome analysis, quantitative PCR (qPCR), and confocal microscopy. PM or DM could not serve as controls because PM is heterogeneous[26] and DM lacks $CD8^+$-mediated immunopathological features. We found that the attacked muscle fibers in sIBM differentially overexpressed members of the interferon (IFN) γ signaling cascade. The signature of these molecular changes suggests that they are induced by locally secreted pro-inflammatory cytokines and, therefore, are a consequence, rather than the cause, of the focal inflammatory attack. In contrast, the ubiquitous up-regulation of HLA-I on all IBM myofibers seems to be independent of IFN-γ–mediated signaling and, therefore, triggered before inflammation by as yet unknown mechanisms.

Materials and Methods

Patients and Healthy Controls

Muscle biopsy specimens were obtained from five patients with sIBM (IBM-1 to IBM-5) and three healthy controls (C-1 to C-3) (Table 1). IBM biopsy samples were obtained at the Neuromuscular Laboratory, Mayo Clinic, Rochester, MN (A.G.E.). The study was approved by the local Institutional Review Board (approval no. 1278–03). Patients' consent was obtained according to the Declaration of Helsinki.[27] None of the five patients with IBM had received prior anti-inflammatory treatment. The diagnosis of definitive IBM was made according to published criteria.[28] Congophilic deposits were visualized in Congo red–stained sections viewed under rhodamine optics.

Three individuals who had clinically presented with nonspecific myalgia, but had normal serum creatine kinase values and normal diagnostic biopsy findings (H.L., University of Munich, Munich, Germany), served as controls. C-1 had clinically silent leukocytosis with slight C-reactive protein elevation at biopsy. All muscle blocks were stored at −80°C. We did not include healthy individuals. For the experiments performed herein, it is absolutely essential that the samples are shock frozen immediately after surgery because otherwise the RNA quality will not be sufficient anymore. RNA, in contrast to DNA or proteins, is degraded rapidly. Therefore, we were limited to diagnostic biopsy material. Samples from autopsy cases or from accidents would not fulfill the listed requirements.

Antibodies

The following antibodies were used in this study. Mouse anti-human CD8α antibody clone LT8 (Serotec, Oxford, UK), which we had previously labeled with the

Cy3-mAb Labeling Kit (GE/Amersham, Freiburg, Germany), was used at 2 μg/mL. Mouse anti-human HLA–avidin-biotin complex (ABC) antibody clone W6/32 (directly labeled with Alexa 488 by the manufacturer; AbD Serotec, Düsseldorf, Germany) was used at 0.5 μg/mL. Rabbit anti-human IFNGR2 antibody, polyclonal (order no. HPA001535; Sigma, Deisenhofen, Germany), was used at 1.6 μg/mL with a goat anti-rabbit Alexa 594–labeled secondary antibody (order no. A-11037; Invitrogen, Darmstadt, Germany) at 4 μg/mL. When unlabeled mouse anti-human CD8α antibody clone LT8 was used (dilution, 10 μg/mL; Serotec), a secondary goat anti-mouse Alexa 488–labeled antibody (order no. A-11029; Invitrogen) was used at 2 μg/mL. For negative controls, we used isotype-matched IgGs [mouse IgG1, order no. 555746 (BD Pharmingen, Heidelberg, Germany); mouse IgG2a, order no. MCA929XZ (AbD Serotec)] for monoclonal antibodies and purified IgG (IgG from rabbit serum, order no. I5006; Sigma) for polyclonal antibodies.

Laser Microdissection

Before the experiments, the RNA quality of each biopsy was assessed by Agilent Bioanalyzer 2100 following the recommendations of the manufacturer (Agilent Technologies, Palo Alto, CA). RNA was heat denatured at 70°C and diluted to concentrations of 5 to 15 ng/μL. RNA, 1 μL, was then used for the Agilent Bioanalyzer chip (Agilent Technologies, Böblingen, Germany). We used a staining and laser microdissection protocol similar to our previously published method.[29] Briefly, 10-μm cryostat sections from muscle biopsy specimens of patients 1 to 5 and healthy controls 1 to 3 were double stained for CD8α and HLA-ABC with the antibodies previously described. To inhibit RNase activity, all aqueous solutions were pretreated with diethylpyrocarbonate and contained 3 U/μL Protector RNase inhibitor (Roche, Mannheim, Germany) and 2% purified bovine serum albumin (B4287; Sigma). Sections were mounted on positron emission tomographic films (P.A.L.M. Microlaser, Bernried, Germany) that had previously been baked at 180°C for 4 hours, UV irradiated, and coated with poly-L-lysine. Mounted sections were stored at −80°C. After drying in a desiccator, rehydrating in PBS for 10 seconds, and blocking by PBS with 2% bovine serum albumin for 3 minutes, the sections were co-incubated for 5 minutes with the Cy-3–labeled anti-CD8α antibody and the Alexa 488–labeled anti-HLA-ABC antibody. This protocol preserves RNA to a large extent (see Supplemental Figure S1 at *http://ajp.amjpathol.org*). The tissue was then rinsed with PBS and immediately imaged using a P.A.L.M. Microbeam-Z microscope (P.A.L.M. Microlaser, Bernried, Germany). We defined a myofiber as being attacked when at least three $CD8^+$ T cells were clearly adhering to the myofiber or at least one $CD8^+$ T cell was invading the fiber. We focused on fibers that were surrounded and superficially invaded by inflammatory cells, avoiding fibers that were deeply invaded. A nonattacked myofiber was defined as such if no $CD8^+$ T cells could be seen in the proximity (Figure 1, A and B). Intermediate myofibers not corresponding to either category were not sampled. The fibers were dissected from transversally cut biopsy sections. When dissecting the myofiber content, we left a safety margin, avoiding contamination with surrounding and superficially invading immune cells (Figure 1, C and D). The specimens were examined within 10 minutes after staining for attacked and nonattacked myofibers, which were marked electronically and subsequently microdissected and laser pressure catapulted into respective reaction tubes (either attacked or nonattacked) containing 20-μL TRIzol (Invitrogen), which were then immediately stored on dry ice. Because of a strong variability in myofiber diameter typically seen in sIBM, we chose to sample equal areas rather than equal numbers of myofibers. The area of each collected myofiber (automatically calculated by the P.A.L.M. software, P.A.L.M. Microlaser) was recorded, and a total of 100,000-μm^2 myofiber area was collected from each patient with sIBM (attacked and nonattacked) and each control subject. To minimize contamination with inflammatory cells, we assessed the dried sections for artifacts by comparing them with

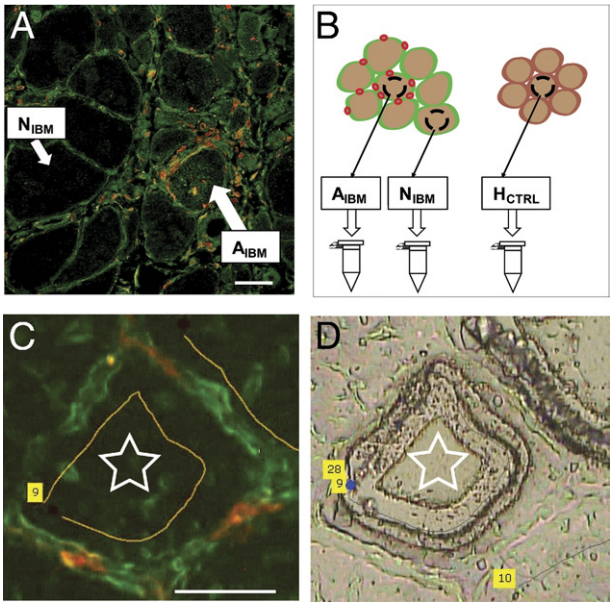

Figure 1. Experimental approach for separate analysis of attacked and nonattacked myofiber subsets in sIBM. **A:** The focal nature of inflammatory infiltrates in IBM. Muscle tissue was stained with anti-CD8 (red) and anti-HLA-ABC (green) antibodies, as described in *Materials and Methods*. **A** shows a confocal image, **C** shows unembedded dry tissue. All myofibers are HLA-ABC positive, but only some are attacked by $CD8^+$ T cells (A_{IBM}), whereas others are spared (N_{IBM}). **B:** Myofibers in direct contact with at least three $CD8^+$ T cells or invaded by at least one $CD8^+$ T cell were defined as A_{IBM}. Myofibers not in contact with any $CD8^+$ T cells were defined as N_{IBM}. Ambiguous myofibers were not sampled. Laser-capture microdissection was used to pressure catapult the different types of myofibers into collecting tubes. In total, 100,000 μm^2 of A_{IBM} and N_{IBM} myofibers was sampled from each patient with sIBM, as was the same amount of H_{CTRL} myofibers from each control subject. **C:** Double immunostaining for HLA-ABC (green) and CD8 (red), according to the protocol described in *Materials and Methods*. Only myofiber tissue (**star**) was isolated, avoiding surrounding lymphocytes (red). **D:** Corresponding bright-light image after the myofiber was dissected and catapulted out of the tissue. **C** and **D:** The numbers in the yellow fields refer to apparatus parameters. Scale bars = 50 μm (**A** and **C**).

embedded tissue (stained under the same conditions and embedded with Fluorescent Mounting Medium; Dako, Glostrup, Denmark). Moreover, we checked for possible contamination by examining our microarray data for the expression of lymphocyte-, monocyte-, and macrophage-specific transcripts (see Supplemental Table S1 at *http://ajp.amjpathol.org*).

RNA Isolation and Linear Transcriptome Amplification

After obtaining 100,000 μm^2 of each group of myofibers, the samples were pooled according to their classification. RNA was then extracted using the TRIzol method, with some modifications as recommended by the linear amplification protocol. Three rounds of linear T7-based transcriptome amplification were performed using the ExpressArt-mRNA Amplification Kit, Pico Version (AmpTec, Hamburg, Germany), according to the instructions of the supplier, with the following exceptions: for synthesis of the first cDNA strand, the master mix was prewarmed at 45°C, and 1 μL of RNase R was added to each reaction for the RNA removal step. The resulting yields of amplified RNA (aRNA) were between 30 and 40 μg, derived from $<$10 ng of input total RNA.

Microarray Hybridization and Analysis

Amplified cDNA, 15 μg, was biotinylated and concomitantly transcribed into aRNA using the BioArray High Yield RNA labeling kit (Enzo Life Sciences, Plymouth Meeting, PA). Biotinylated aRNA was hybridized to HG U133 GeneChip arrays (Affymetrix, High Wycombe, UK). All chips were normalized using the robust multiarray average or the GeneChip robust multiarray average procedure in R packages from Bioconductor (Fred Hutchinson Center, Seattle, WA) (*http://www.bioconductor.org*, last accessed December 2008). For each probe set, the q values were calculated.[30] The q values mirror the false discovery rate and illustrate the degree of heterogeneity between different samples (ie, herein, between different patients). Thus, a low q value reflects a high significance of a particular expression change across all samples. To achieve a high concordance across all patients, we considered only transcripts with a q value of $\leq$20%.

TaqMan Real-Time qPCR

Expression levels of the following genes were measured in all 13 samples (attacked and nonattacked myofibers from each of the five patients and C-1 to C-3) by real-time qPCR using the 5700 Real-Time PCR System (Applied Biosystems, Foster City, CA): *HLA-A*, *HLA-B*, *HLA-C*, *HLA-E*, *HLA-F*, *HLA-G*, IFN-γ receptor α chain (*IFNGR1*), IFN-γ receptor β chain (*IFNGR2*), *STAT1*, class II transactivator (*CIITA*), proteasome subunit β-type 8 (*PSMB8*), *HLA-DRA*, *HLA-DRB*, *HLA-DPA*, *HLA-DPB*, *HLA-DQA*, *HLA-DQB*, *CCL5*, and *STAT3*. aRNA was reverse transcribed into cDNA using primer D from the ExpressArt-mRNA Amplification Kit. Three replicates per sample were assayed for each gene in a 96-well format plate. For data normalization across samples, cyclophilin was used as a housekeeping gene. Normalization of the C_T values of each gene and determination of fold changes in gene expression were calculated according to the comparative C_T method, also

Table 2. Genes Analyzed with TaqMan qPCR

Gene	TaqMan qPCR primers/probes
HLA-A	Fwd: 5′-CTGAGATGGGAGCTGTCTTC-3′
	Rev: 5′-CTATCTGAGCTCTTCCTCCT-3′
	P: 5′-FAM-GTAAAGTGTGAGACAGCTGCCTTG-TAMRA-3′
HLA-B	Fwd: 5′-CTGAGATGGGAGCCGTCTT-3′
	Rev: 5′-CTCCTTTTCCACCTGAACTC-3′
	P: 5′-FAM-GAGCTTGAAAAGCCTGAGAGAGC-TAMRA-3′
HLA-C	Fwd: 5′-GAGCTGGGAGCCATCTTCC-3′
	Rev: 5′-CTGTTGCTGCACGCAGCCT-3′
	P: 5′-FAM-CCATCATGGGCATCGTTGCTGG-TAMRA-3′
HLA-E	Fwd: 5′-GTCACCCTGAGATGGAAGC-3′
	Rev: 5′-CTTGGATCTGTGGTCTCTGG-3′
	P: 5′-FAM-CCATCGTGGGCATCATTGCTGG-TAMRA-3′
HLA-F	Fwd: 5′-CCTCCAAAGGCACACGTTG-3′
	Rev: 5′-GATAGAAACAGAGGGAGCTAC-3′
	P: 5′-FAM-CAAGACACACGTGACCCACCAC-TAMRA-3′
HLA-G	Fwd: 5′-CCACAGATACCTGGAGAACG-3′
	Rev: 5′-GATCATACTGACCTGGCAGC-3′
	P: 5′-FAM-CAAGACACACGTGACCCACCAC-TAMRA-3′
IFNGR1	Fwd: 5′-CATCACGTCATACCAGCCATTT-3′
	Rev: 5′-CTGGATTGTCTTCGGTATGCAT-3′
	P: 5′-FAM-GGTCTGTGAAGAGCCGTTGTCTC-TAMRA-3′
IFNGR2	Fwd: 5′-CCACCAAGCATCCCATTACA-3′
	Rev: 5′-CCTTGGACAAGGACAGCTC-3′
	P: 5′-GACCCAACTCAGCCCATCTTAGA-3′
STAT1	Fwd: 5′-GAGCAGGTTCACCAGCTTTATG-3′
	Rev: 5′-GAAAACGGATGGTGGCAAATG-3′
	P: 5′-FAM-CAAGACTGGGAGCACGCTGCCAA-TAMRA-3′
CIITA	Fwd: 5′-ACGCCCTGCTGGGTCC-3′
	Rev: 5′-AACTCCATGGTGGCACACTG-3′
	P: 5′-FAM-ACCTGTCAGAGCCCCAAGGCAGC-TAMRA-3′
PSMB8	Fwd: 5′-GTCCTACATTAGTGCCTTACG-3′
	Rev: 5′-GATAGTACAGCCTGCATTCC-3′
	P: 5′-FAM-GCTGTGCAGACTGTCAGTAC-TAMRA-3′
HLA-DRA	Fwd: 5′-GGCTTGGATGAGCCTCTTC-3′
	Rev: 5′-GGACCATCTTCATCATCAAGG-3′
	P: 5′-FAM-CAAGCACTGGGAGTTTGATGCTC-TAMRA-3′
HLA-DRB	Fwd: 5′-GGAGAGGTTTACACCTGCC-3′
	Rev: 5′-GCAAGATGCTGAGTGGAGTC-3′
	P: 5′-FAM-GAATGGAGAGCACGGTCTGAATC-TAMRA-3′
HLA-DPA	Fwd: 5′-CACAAGTTCCATTACCTGACC-3′
	Rev: 5′-GAGCAAGAAAGTTCAACGAGG-3′
	P: 5′-CTTCTATGACTGCAGGGTGGAGC-3′
HLA-DPB	Fwd: 5′-GGAGTGGAAGGCACAGTCT-3′
	Rev: 5′-GAGCAAGAAAGTTCAACGAGG-3′
	P: 5′-CGGAGTAAGACATTGACGGGAGC-3′
HLA-DQA	Fwd: 5′-CACCAAGGGCCATTGTGAAT-3′
	Rev: 5′-CCAGAGAATAGTGCTAGGTC-3′
	P: 5′-FAM-CCATCTACAGGAGCAGAAGAATGG-TAMRA-3′
HLA-DQB	Fwd: 5′-CCAGAGCAAGATGCTGAGTG-3′
	Rev: 5′-GTGCAGAAGCCCTTTCTGAC-3′
	P: 5′-FAM-GGCTGGGCCTTATCATCCGTCAA-TAMRA-3′
CCL5	Applied Biosystems assay ID Hs00174575_m1
STAT3	Applied Biosystems assay ID Hs01047580_m1
PPIA	Applied Biosystems no. 4333763
GAPDH	Applied Biosystems no. 4333764

Classic and nonclassic *HLA-I* genes were analyzed, as were the major *HLA-II* genes *DR*, *DP*, and *DQ*. Moreover, we examined the expression of genes downstream of IFN-γ. Forward and reverse primers, and FAM/TAMRA-labeled probes, are listed. All primer/probe sets were designed by us, with the exceptions of IFNGR1[33] and CIITA.[34]

Fwd, forward; GAPDH, glyceraldehyde-3-phosphate dehydrogenase; P, probe; PPIA, cyclophilin; Rev, reverse.

Table 3. Microarray Data: Transcripts Most Significantly Regulated across All Patients and Controls

		Raw expression values				Fold change		
Probe set ID	Gene title	A_{IBM}	N_{IBM}	H_{CTRL}	q value (%)	A_{IBM}/ H_{CTRL}	A_{IBM}/ N_{IBM}	N_{IBM}/ H_{CTRL}
205132_at	Actin, α, cardiac muscle 1	9926.55	5275.13	338.44	0.00	29.33	1.88	15.59
201891_s_at*	β-2-Microglobulin	12,436.09	11,093.17	1570.33	0.00	7.92	1.12	7.06
216526_x_at*	MHC, class I, B; MHC, class I, C; MHC class I polypeptide-related sequence A; MHC class I polypeptide-related sequence B	8959.71	7976.71	705.27	0.00	12.70	1.12	11.31
209140_x_at*	MHC, class I, B; MHC, class I, C; MHC class I polypeptide-related sequence A; MHC class I polypeptide-related sequence B	9521.62	7469.66	297.92	0.00	31.96	1.27	25.07
217456_x_at*	MHC, class I, E	1503.90	827.43	75.69	0.00	19.87	1.82	10.93
200905_x_at*	MHC, class I, E	3383.98	1638.89	57.90	0.00	58.44	2.06	28.30
221875_x_at*	MHC, class I, F	1959.54	1293.23	101.36	0.00	19.33	1.52	12.76
211529_x_at*	MHC, class I, G	250.88	163.19	12.87	0.00	19.49	1.54	12.68
209040_s_at*	Proteasome (prosome, macropain) subunit, β type, 8 (large multifunctional peptidase 7)	1751.19	613.20	4.05	0.00	432.37	2.86	151.40
202296_s_at	RER1 retention in endoplasmic reticulum 1 homolog (*Saccharomyces cerevisiae*)	16.24	23.27	706.64	0.00	0.02	0.70	0.03
200887_s_at*	STAT 1, 91 kDa	7963.49	6296.56	94.89	0.00	83.92	1.26	66.35
AFFX-HUMISGF3A/ M97935_3_at*	STAT 1, 91 kDa	1928.89	1828.85	34.57	0.00	55.80	1.05	52.91
221087_s_at	Apolipoprotein L, 3	605.96	373.82	25.70	5.12	23.58	1.62	14.55
208812_x_at*	MHC, class I, C	9337.37	6540.77	430.46	5.12	21.69	1.43	15.19
214459_x_at*	MHC, class I, C	6556.01	4679.25	371.30	5.12	17.66	1.40	12.60
204806_x_at*	MHC, class I, F	753.67	512.69	59.87	5.12	12.59	1.47	8.56
211071_s_at	Myeloid/lymphoid or mixed-lineage leukemia (trithorax homologue, *Drosophila*), translocated to 11	4511.40	2944.13	205.20	5.12	21.99	1.53	14.35
202237_at	Nicotinamide *N*-methyltransferase	1944.88	1365.55	21.27	5.12	91.44	1.42	64.20
212845_at	Sterile α motif domain containing 4A	22.95	44.53	554.77	5.12	0.04	0.52	0.08
215076_s_at	Collagen, type III, α 1 (Ehlers-Danlos syndrome type IV, autosomal dominant)	6542.53	3846.48	12.69	8.84	515.45	1.70	303.05
213932_x_at*	MHC, class I, A	9857.13	7352.34	2127.78	8.84	4.63	1.34	3.46
201137_s_at*	MHC, class II, DP β 1	1817.92	684.36	37.08	8.84	49.02	2.66	18.46
225061_at	DnaJ (Hsp40) homologue, subfamily A, member 4	1906.51	1525.02	29.68	11.67	64.24	1.25	51.39
211528_x_at*	MHC, class I, G	195.97	149.47	16.23	11.67	12.08	1.31	9.21
200814_at*	Proteasome (prosome, macropain) activator subunit 1 (PA28 α)	4007.01	3496.38	405.11	11.67	9.89	1.15	8.63
232500_at	Chromosome 20 open reading frame 74	1047.84	210.09	12.61	14.41	83.07	4.99	16.66
217436_x_at*	MHC, class I, J (pseudogene)	141.93	114.16	19.59	14.41	7.24	1.24	5.83
226470_at	γ-Glutamyltransferase 7	51.17	51.41	1893.54	16.21	0.03	1.00	0.03
228098_s_at	Myosin regulatory light chain interacting protein	794.08	85.92	27.30	16.21	29.09	9.24	3.15
200743_s_at	Tripeptidyl peptidase I	1741.52	1749.31	337.65	16.21	5.16	1.00	5.18
238431_at	Transcribed locus	1251.44	347.59	22.14	20.02	56.52	3.60	15.70
215313_x_at*	MHC, class I, A	11,623.07	9764.78	968.10	20.02	12.01	1.19	10.09
204070_at	Retinoic acid receptor responder (tazarotene induced) 3	3065.52	1516.95	88.87	20.02	34.49	2.02	17.07
209118_s_at	Tubulin, α 1a	1608.79	1037.65	48.98	20.02	32.85	1.55	21.19

Raw expression values are provided along with fold expression changes showing regulation of transcripts in A_{IBM} vs H_{CTRL}, A_{IBM} vs N_{IBM}, and N_{IBM} vs H_{CTRL}. The q value mirrors the false discovery rate. The lower the q value, the higher the significance of the results across all samples (see *Materials and Methods*). Herein, we show transcripts that were expressed with a q value of ≤20%.

*Among these 34 transcripts, 19 can be attributed to components of the classic and nonclassic *HLA-I*, *HLA-II*, *IFN-γ*–inducible genes and immunoproteasome components.

MHC, major histocompatibility complex; RER, retention in endoplasmic reticulum.

known as the $2^{-\Delta C_T}$ method.[31,32] For some genes, TaqMan gene expression assays (Applied Biosystems) were used; others were analyzed using custom-made primers and probes (Metabion, Martinsried, Germany). Table 2 lists the primers and probes used in this study.

Histological Features and Confocal Microscopy

To demonstrate $CD8^+$ T-cell interaction with HLA-I–positive myofibers, we used 10-μm cryosections fixed in ice-cold acetone. To block nonspecific binding, sections

were incubated with 2% bovine serum albumin and 2% mouse serum in PBS. Then, we stained for CD8α and HLA-ABC using the antibodies previously described. To confirm IFNGR2 expression on the protein level, we fixed the tissue in 4% paraformaldehyde at room temperature and washed with PBS, then blocked unspecific binding with 2% bovine serum albumin–2% goat serum in PBS, and subsequently stained for CD8α (same as previously described, unlabeled) and rabbit anti-human IFNGR2 antibody (Sigma). After washing in PBS, sections were incubated with goat anti-mouse Alexa 488–labeled antibody and goat anti-rabbit Alexa 594–labeled antibody (both from Invitrogen). For negative controls, we used isotype-matched IgGs (mouse IgG1 for anti-CD8 and mouse IgG2a for anti-HLA-ABC) for monoclonal antibodies and purified IgG (rabbit IgG) for polyclonal antibodies. The staining was visualized using a Zeiss Axiovert 200M inverted microscope (Zeiss, Göttingen, Germany). For confocal microscopy, a Leica TCS SP2 system was used (Leica Microsystems, Wetzlar, Germany). For image analysis, we used the ImageJ software written by Wayne Rasband at the US NIH, version 1.42m (*http://rsbweb.nih.gov/ij/index.html*, last accessed September 2010).

Quantitative Analysis of IFNGR2 Signal Distribution

Cryosections were stained for IFNGR2 and CD8 and imaged as previously described. Myofibers were photographically documented and classified into four groups according to their extent of membrane circumference positivity for IFNGR2: group 1, >80%; group 2, 50% to 80%; group 3, 20% to 50%; and group 4, <20%. For each myofiber, we counted the number of adjacent $CD8^+$ T cells and calculated the medians. Two investigators (J.I. and Ingrid Eiglmeier) independently performed this analysis for each patient. A Mann-Whitney *U*-test was performed to determine whether the medians of adjacent $CD8^+$ T cells of group 1 (>80% IFNGR2 positivity) and group 4 (<20% IFNGR2 positivity) differed significantly. The two-tailed *P* value was calculated, as was the Mann-Whitney *U*-test value. This analysis was performed for four of five patients with sIBM because of lack of biopsy material from patient 4.

Results

Hints from Microarray Analysis of Attacked and Nonattacked Myofibers

We isolated A_{IBM}, N_{IBM}, and H_{CTRL} myofibers from five patients and three control individuals, as described in *Materials and Methods* and illustrated in Figure 1. At least 100,000 μm^2 of total myofiber area was isolated from each fiber subset of each patient and from each control. We amplified RNA from these laser-microdissected samples and hybridized the aRNA to HG U133 GeneChip microarrays. The microarray data were cross-checked for inadvertent sampling of inflammatory cells (see Supplemental Table S1 at *http://ajp.amjpathol.org*). We focused on transcripts that were regulated with q values of ≤20% (Table 3) to ensure that interpatient variation is minimized. Of the 34 transcripts with a q value of ≤20%, 19 belonged to *HLA-I*, *HLA-II*, or inflammatory signaling genes. Next, we explored whether these molecules are differentially expressed in A_{IBM} versus N_{IBM} versus H_{CTRL} myofibers. Of these 34 transcripts, six were polymorphic HLA-I (ie, HLA-A, HLA-B, or HLA-C). Both A_{IBM} and N_{IBM} myofibers showed a strong up-regulation of HLA-ABC expression compared with H_{CTRL} myofibers (average fold change for A_{IBM}/H_{CTRL} = 16.78, N_{IBM}/H_{CTRL} = 12.95, and A_{IBM}/N_{IBM} = 1.29). Moreover, seven nonpolymorphic HLA-I

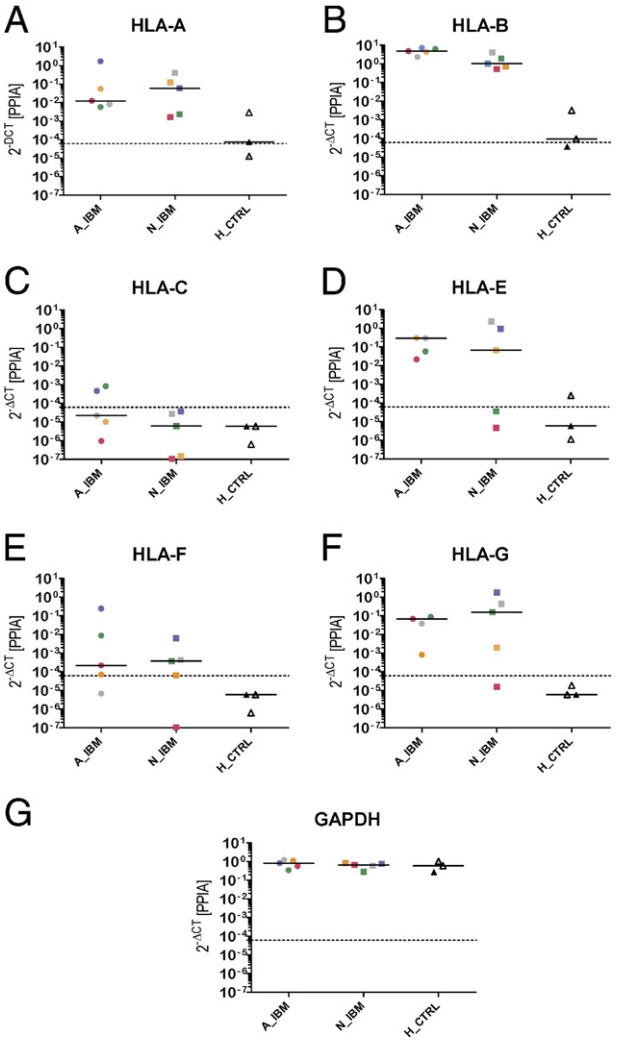

Figure 2. Comparison of transcript levels in attacked, nonattacked, and healthy control myofibers using TaqMan qPCR. Relative expression values were calculated using the $2^{-\Delta CT}$ method with cyclophilin as the endogenous control. Each symbol represents the mean of triplicate experiments performed on one sample. Five A_{IBM} samples (circles), five N_{IBM} samples (squares), and three H_{CTRL} samples (triangles) were included in the study. Colors correspond to individual patients (IBM-1, pink; IBM-2, green; IBM-3, gray; IBM-4, blue; IBM-5, yellow) and controls (C-1, white; C-2, gray; C-3, black), and medians are shown for each subset. Dashed line, detection limit. The following are shown: HLA-A (**A**), HLA-B (**B**), HLA-C (**C**), HLA-E (**D**), HLA-F (**E**), HLA-G (**F**), and glyceraldehyde-3-phosphate dehydrogenase (GAPDH) (**G**). Data for HLA-E and HLA-G from A_{IBM} of patient 4 were out of range (>100) and are omitted. HLA-A and HLA-B were strongly up-regulated in both attacked and nonattacked sIBM myofibers. The nonclassic HLA (ie, HLA-E, HLA-F, and HLA-G) displayed a pattern similar to that of HLA-A and HLA-B. GAPDH was used as an additional endogenous control. As expected, its expression pattern largely mirrors that of cyclophilin in that it is unchanged in all samples.

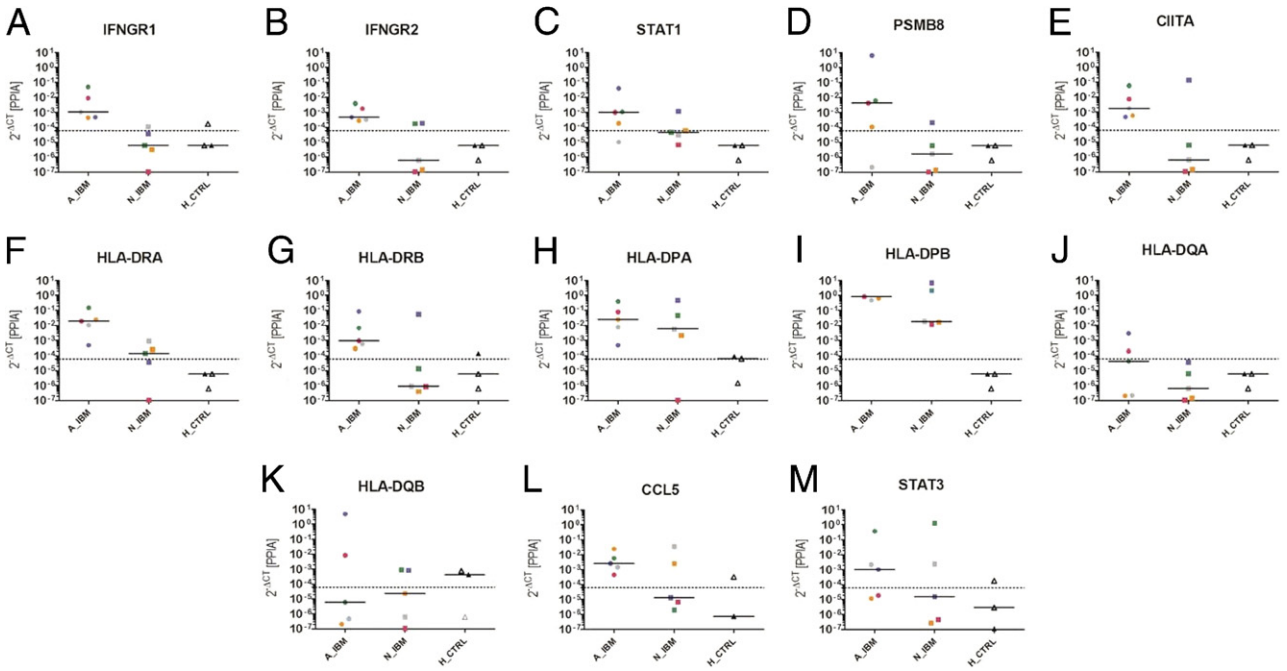

Figure 3. Comparison of transcript levels in attacked, nonattacked, and healthy control myofibers using TaqMan qPCR. Relative expression values were calculated using the $2^{-\Delta CT}$ method with cyclophilin as the endogenous control. The following are shown: IFNGR1 (**A**), IFNGR2 (**B**), STAT1 (**C**), PSMB8 (**D**), CIITA (**E**), HLA-DRA (**F**), HLA-DRB (**G**), HLA-DPA (**H**), HLA-DPB (**I**), HLA-DQA (**J**), HLA-DQB (**K**), CCL5 (**L**), and STAT3 (**M**). The legend to Figure 2 provides a detailed explanation of all symbols. IFNGR1, IFNGR2, STAT1, CIITA, and PSMB8, as well as HLA-DRA and HLA-DRB, were overexpressed in attacked myofibers compared with nonattacked myofibers and healthy controls. For HLA-DP, the difference between attacked and nonattacked myofibers was less pronounced. HLA-DQ was only detectable in two of five patients with sIBM.

(ie, HLA-E, HLA-F, or HLA-G) transcripts were up-regulated, with low q values (average fold change for A_{IBM}/H_{CTRL} = 23.63, N_{IBM}/H_{CTRL} = 13.74, and A_{IBM}/N_{IBM} = 1.62).

Two probe sets of STAT1, a mediator of IFN signaling, were regulated, with a q value of 0%, thus being highly significant across all patients. STAT1 was strongly expressed in A_{IBM} and N_{IBM} and undetectable in H_{CTRL}. HLA-DPB1 was the only HLA-II transcript with a q value <20%. In contrast to HLA-I, HLA-DPB1 was up-regulated 2.66-fold in A_{IBM} versus N_{IBM} myofibers. PSMB8, a major constituent of the immunoproteasome, had a q value of 0% as well and was differentially regulated in A_{IBM} versus N_{IBM} (fold change = 2.86).

Several transcripts important for inflammatory signaling and antigen presentation were overexpressed in global microarrays from sIBM biopsy specimens by other researchers (see Supplemental Table S2 at *http://ajp.amjpathol.org*). Although only some of the transcripts had significantly low q values, our results allow us to attribute these regulation patterns to specific myofiber subsets. On the other hand, Ig genes were absent in our myofiber-specific microarray studies (see Supplemental Table S1 at *http://ajp.amjpathol.org*). This ensures that cells of the B lineage, and not myofibers, are the source of Igs in sIBM tissue.[35,36]

TaqMan qPCR Confirms Global HLA-I Up-Regulation in sIBM Muscle Fibers

We analyzed aRNA from laser-microdissected A_{IBM}, N_{IBM}, and H_{CTRL} myofibers using TaqMan qPCR. Relative expression values were calculated for all TaqMan results using the $2^{-\Delta C_T}$ method.[31,32]

We found that all members of the HLA-I family were up-regulated in both A_{IBM} and N_{IBM} compared with H_{CTRL} myofibers (Figure 2). This agrees with our microarray data and with previous immunohistological studies[21] and supports the overall validity of our experimental approach.

Differential Regulation of IFN-γ Downstream Signaling Pathways

We found several IFN-γ–inducible molecules to be differentially up-regulated in A_{IBM} versus N_{IBM} and H_{CTRL} myofibers. To see whether myofibers are susceptible to IFN-γ, we analyzed the expression of both chains of IFNGR and its major downstream mediator STAT1 in A_{IBM} versus N_{IBM} and H_{CTRL} myofibers with TaqMan qPCR. Both IFNGR1 and IFNGR2 were overexpressed in A_{IBM}. In N_{IBM} and H_{CTRL} myofibers, the expression of both IFNGR chains ranged below the detection limit in most cases (Figure 3, A and B). STAT1 was up-regulated in A_{IBM} and below the detection limit in N_{IBM} and H_{CTRL} (Figure 3C). Two other major downstream effector proteins of IFN-γ, the immunoproteasome component PSMB8[37] and CIITA,[38] were up-regulated in A_{IBM} compared with N_{IBM} and H_{CTRL} (Figure 3, D and E). In one patient, the levels of all three downstream transcripts (ie, STAT1, PSMB8, and CIITA) were particularly high compared with the other patients. This reflects a certain interindividual variability that is to be expected in such a cohort.

Next, we investigated whether IFN-γ cascade up-regulation results in effective HLA-II overexpression in A_{IBM}. We looked at the expression of the respective α and β chains of HLA-DR, HLA-DP, and HLA-DQ. HLA-DRA and HLA-DRB were up-regulated in A_{IBM} compared with N_{IBM} and H_{CTRL} myofibers (Figure 3, F and G). In the case of HLA-DPA and HLA-DPB, the difference in overexpression between A_{IBM} and N_{IBM} was less striking (Figure 3, H and I). HLA-DQA and HLA-DQB showed the same tendency, albeit with lower expression levels (Figure 3, J and K).

Because tumor necrosis factor (TNF)-α induces chemokine ligand (CCL) 5 [regulated on activation normal T-cell expressed and secreted (RANTES)] via STAT3 in vascular smooth muscle cells and many other nonlymphoid cell types,[39] we investigated the transcriptional activity of the CCL5-STAT3 system in our laser-microdissected myofiber subsets from patients with sIBM. Although RANTES and STAT3 levels were generally low, and the expression patterns were heterogeneous across all patients and controls, median values indicate a tendency for higher CCL5 expression in attacked myofibers compared with nonattacked myofibers and healthy controls (Figure 3, L and M).

Confocal Microscopy Confirms Differential IFNGR2 Expression in A_{IBM} versus N_{IBM} Myofibers

On binding of IFN-γ, IFNGR1 is internalized in a complex with STAT1, whereas IFNGR2, also known as the inducible chain of the IFN-γ receptor, remains on the cell surface.[40] To evaluate IFNGR2 expression on the protein level, we double stained cryosections from five patients with sIBM and three controls for IFNGR2 and CD8. We found that a proportion of myofibers of patients with sIBM stained positive for IFNGR2. The IFNGR2 was not uniformly distributed in patients with sIBM. Some myofibers were positive for IFNGR2 along their entire surface. Other myofibers showed only partial segmental membrane staining, and yet others were entirely negative. This variability of IFNGR2 membrane staining was similar in all five patients with sIBM who were included in our study. By

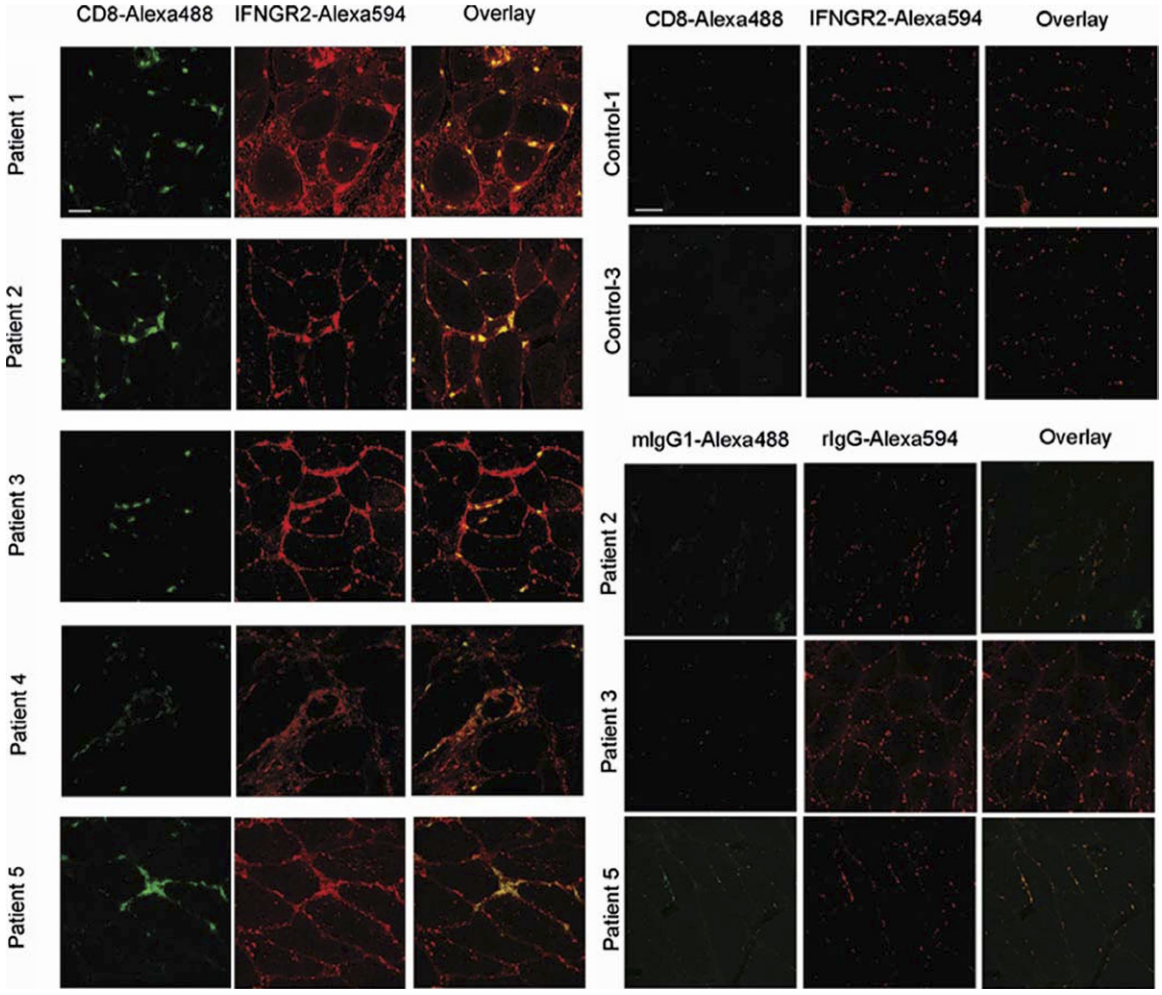

Figure 4. IFNGR2 expression on the protein level in patients with sIBM and healthy controls. IFNGR2 (Alexa 594 in red) and CD8 (Alexa 488 in green) were stained as described in *Materials and Methods* and visualized with confocal microscopy. Technical controls were performed with rat IgG (rIgG) for anti-IFNGR2 antibody and mouse Ig isotype 1 (mIgG1) for anti-CD8 antibody under identical experimental conditions. **Left** to **right:** Images are organized as follows: green channel (CD8 or respective control), red channel (IFNGR2 or respective control), and overlay.

contrast, myofibers from healthy controls did not stain positive for IFNGR2 (Figure 4).

We then asked whether the extent of IFNGR2 expression might be related to the extent of inflammatory changes around individual fibers. To this end, we classified myofibers into four groups according to the extent of IFNGR2 surface expression as follows: group 1, >80%; group 2, 50% to 80%; group 3, 20% to 50%; and group 4, <20% surface staining (Figure 5). Control sections stained in the same experiment were uniformly negative for IFNGR2 (Figure 4). Two independent observers (J.I. and Ingrid Eiglmeier) evaluated the numbers of attacking $CD8^+$ T cells that were in direct contact with each myofiber for each classified myofiber (Figure 6). A Mann-Whitney *U*-test was performed to determine whether the distributions of adjacent $CD8^+$ T-cell numbers per myofiber in groups 1 and 4 differed significantly in all analyzed patients (Figure 6). In patient IBM-1, the median $CD8^+$ T-cell numbers were 5 and 1 (observer Ingrid Eiglmeier: Mann-Whitney *U*-test = 9.5, $P < 0.0001$) and 6 and 1 (observer J.I.: Mann-Whitney *U*-test = 5.5, $P < 0.0001$), respectively. In patient IBM-2, the median $CD8^+$ T-cell numbers were 4 and 0 (observer I.E.: Mann-Whitney *U*-test = 0, $P < 0.0278$) and 5 and 0.5 (observer J.I.: Mann-Whitney *U*-test = 0, $P < 0.0223$), respectively. In patient IBM-3, the median $CD8^+$ T-cell numbers were 5 and 1 (observer Ingrid Eiglmeier: Mann-Whitney *U*-test = 3, $P < 0.0072$) and 5.5 and 1 (observer J.I.: Mann-Whitney *U*-test = 0.5, $P < 0.0011$), respectively. In patient IBM-5, the median $CD8^+$ T-cell numbers were 6 and 0 (observer IE: Mann-Whitney *U*-test = 13, $P < 0.0001$) and 7 and 0 (observer J.I.: Mann-Whitney *U*-test = 10.5, $P < 0.0001$), respectively. (All *P* values were two tailed.) The results reveal a positive correlation between the density of the focal inflammatory infiltrate and the extent of IFNGR2 surface expression, indicating that IFNGR2 is up-regulated on myofibers by locally produced pro-inflammatory cytokines.

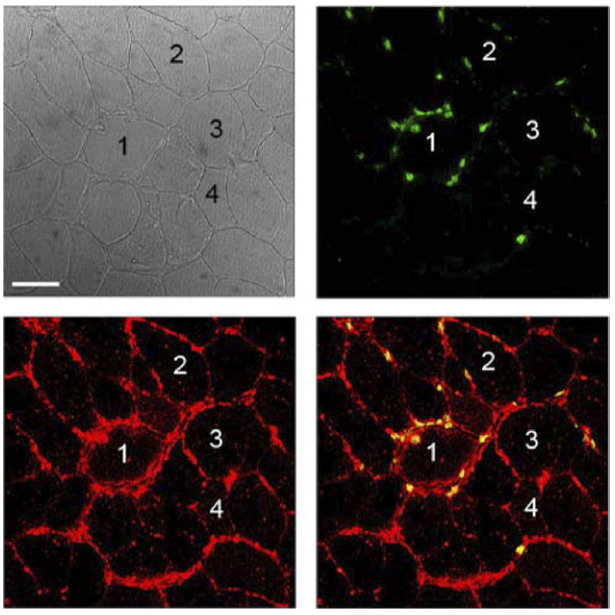

Figure 5. IHC demonstrates differential IFNGR2 expression in patients with sIBM. IFNGR2 (Alexa 594 in red) and CD8 (Alexa 488 in green) were stained as described in *Materials and Methods* and visualized with confocal microscopy. Although some myofibers were strongly positive for IFNGR2 along their entire surface, others were only segmentally positive or negative. The strongly positive myofibers were often heavily attacked by $CD8^+$ T cells. Herein, representative examples from one patient are shown. Four groups were defined according to IFNGR2 membrane positivity: group 1, >80% of the myofiber membrane positive for INFGR2; group 2, 50% to 80% of the myofiber membrane positive for INFGR2; group 3, 20% to 50% of the myofiber membrane positive for INFGR2; and group 4, <20% of the myofiber membrane positive for INFGR2. Images are organized clockwise from **top left** as follows: transmission, green channel (CD8 or respective control), red channel (IFNGR2 or respective control), and overlay. Scale bar = 50 μm.

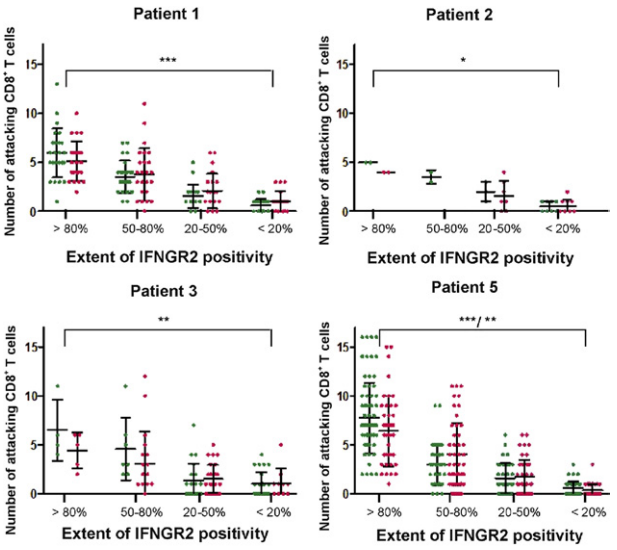

Figure 6. Relationship between extent of membrane positivity for IFNGR2 and number of adjacent $CD8^+$ T cells. Each dot represents an individual myofiber. Each myofiber was assigned to a group according to the criteria discussed in *Results* and in Figure 5, and the number of adjacent $CD8^+$ T cells was counted. In the previously described graphs, the number of adjacent $CD8^+$ T cells was plotted against the respective group for each myofiber. Results from two independent observers (green and pink) are shown side by side. Mann-Whitney *U*-tests were performed to determine statistical significance (*$P < 0.01$, **$P < 0.001$, and ***$P < 0.0001$). Patient IBM-4 was not included because of lack of material for a systematic analysis.

Discussion

In sIBM, essentially all muscle fibers express HLA-I.[6] By contrast, the attacking $CD8^+$ T cells follow a strictly focal pattern. In the present study, we sought to identify differences between the following: A_{IBM}, N_{IBM}, and H_{CTRL}. We focused on the molecular pathways of antigen presentation. We did not investigate PM or DM because PM is heterogeneous[26] and DM lacks $CD8^+$-mediated muscle fiber injury. We found high levels of HLA-I in both A_{IBM} and N_{IBM} myofibers. In contrast, the receptor for IFN-γ was overexpressed in A_{IBM} compared with N_{IBM} myofibers, indicating increased susceptibility of A_{IBM} to IFN-γ downstream signaling.

Ubiquitous Up-Regulation of HLA-I

Most tissues constitutively express HLA-I molecules. Muscle is an exception in that HLA-I is normally undetectable but up-regulated in inflammatory myopathies.[21,24,41] In sIBM, HLA-I expression is essentially ubiquitous on all myofibers. Consistent with this well-

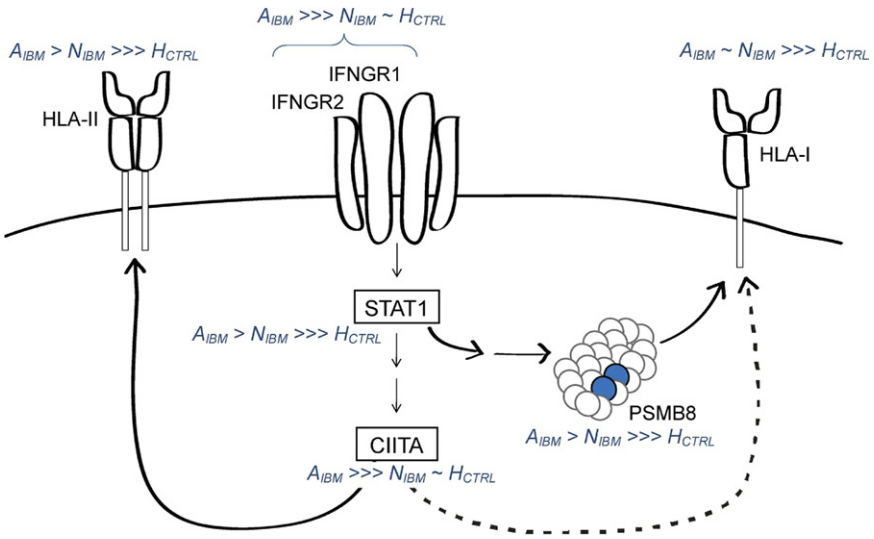

Figure 7. Scheme for changes in the molecular pattern of inflammatory signaling, antigen processing, and presentation in attacked myofibers. HLA-I molecules are up-regulated in all IBM myofibers. We show the pronounced effect of IFN-γ–induced CIITA on HLA-II by a continuous **arrow** and the relatively small effect of CIITA on HLA-I expression (Gobin et al, 1998) as a **dotted arrow**. However, the effect of CIITA cannot be held responsible for the initial IFN-γ–independent and probably ubiquitous HLA-I up-regulation. In A_{IBM}, we found up-regulation of IFN-γ pathway components IFNGR1 and IFNGR2. The response to IFN-γ explains the up-regulation of IFN-γ–inducible genes, such as *STAT1*, *CIITA*, *PSMB8*, and *HLA-II*, in A_{IBM}.

established histological feature, we observed up-regulation of classic and nonclassic HLA-I transcripts in both A_{IBM} and N_{IBM} (Figure 7). This confirms and extends previous observations that nonclassic HLA-G is up-regulated on muscle fibers in inflammatory myopathies.[42] Because up-regulation of HLA-I on sIBM myofibers is independent of the presence of local inflammatory cells,[6] and because it may occur in the absence of an IFN-γ signature (as shown by our present results from N_{IBM}), it appears that HLA-I is induced by unknown triggers upstream of the IFN-γ–related changes. Other inflammatory mediators (eg, TNF-α) may precede and subsequently potentiate the IFN-γ cascade, as suggested by our findings on the up-regulation of CCL5-STAT3 in attacked myofibers, which is a TNF-α–inducible chemokine system.[39] IFN-α is a further important inflammatory mediator implicated in the pathogenesis of inflammatory myopathies. In juvenile DM, IFN-α up-regulated HLA-I and several IFN-γ–inducible genes, possibly through up-regulation of IL1-α/β.[43,44] The interplay between IFN-α and IFN-γ demonstrated in juvenile DM may play a role in sIBM as well.

The nonhistone nuclear protein alarmin high-mobility group box 1 protein may be a further important upstream inducer of HLA-I in sIBM. High-mobility group box 1 protein up-regulation has been demonstrated in myofibers of patients with inflammatory myopathies early in the disease course. Moreover, high-mobility group box 1 protein up-regulated HLA-I on muscle cells *in vitro*.[45]

Another possible explanation for IFN-γ–independent HLA-I induction may be a viral infection, given the known association of inflammatory myopathies with human T-lymphotropic virus I and HIV.[46–48] Moreover, viral infection induced HLA-I on cultured human myoblasts independently of IFN-γ.[49] Although there is no current evidence that HLA-I can be induced by degenerative factors, the HLA-I up-regulation in sIBM might be related to the observed degenerative changes.[50–52] Amyloid-β precursor protein and embryonic myosin variants showed reasonable q values between 20% and 40% (data not shown). These findings, which need to be extended and confirmed in future studies, would be consistent with the concept that inflammatory and degenerative changes in sIBM are mutually related.[53,54] An additional aspect not addressed in our study is the expression of αB-crystallin in so-called X fibers.[55] Previous observations that X fibers are otherwise morphologically normal, and are not (yet?) attacked by inflammatory cells, suggested that αB-crystallin expression is induced in these fibers by an unknown proximal triggering event, perhaps infection with an unknown virus. It will be interesting to apply our microdissection approach to the investigation of X fibers in future studies.

The precise pathogenetic role of HLA-I overexpression remains uncertain. In animal models, overexpression of major histocompatibility complex I was associated with inflammatory and degenerative myopathic changes, possibly related to an endoplasmic reticulum stress response.[56–58] Furthermore, HLA-I expression is definitively a prerequisite for $CD8^+$ T-cell–mediated muscle fiber injury because $CD8^+$ T cells recognize HLA-I–bound antigenic peptides. Previous studies[59] have demonstrated HLA-I up-regulation in human myoblasts incubated by IFN-γ. The difference might be explained by the fact that mature myofibers differ from less differentiated myotubes and myoblasts. However, as supported by our findings, HLA-I is only a necessary, but by no means sufficient, precondition for a $CD8^+$ T-cell–mediated attack, and HLA-I expression alone cannot explain the focal character of inflammation in sIBM.

Up-Regulation of IFN-γ Receptor in Attacked Myofibers

The crucial upstream protein required for initiation of downstream IFN-γ signaling is the IFN-γ receptor, which was expressed by A_{IBM} but not N_{IBM} or H_{CTRL} myofibers by qPCR (Figure 7). When IFN-γ binds to the IFN-γ receptor, the complex of IFN-γ, IFNGR1, and STAT1 translocates into the nucleus while IFNGR2 remains on the cell surface.[40,60] In sIBM muscle, IFNGR2 protein expression,

as demonstrated by immunofluorescence staining, was heterogeneous and related to the presence of inflammatory cells. Quantitative analysis of the relationship between inflammatory cells and segmental IFNGR2 expression revealed a positive correlation between the extent of IFNGR2 surface expression on myofibers and the number of adjacent $CD8^+$ T cells in all patients, confirming our qPCR findings.

Up-Regulation of IFN-γ–Induced Transcripts

An important downstream component of the IFN-γ signaling cascade is STAT1 (Figure 7). A role for STAT1 overexpression has been demonstrated for DM and PM.[61] Our qPCR results revealed that STAT1 is differentially overexpressed in A_{IBM} myofibers, which is consistent with our observation that IFNGR2 is preferentially expressed in A_{IBM} myofibers.

CIITA (Figure 7) is the most important transcription factor for the induction of HLA-II.[62] To some extent, CIITA can induce HLA-I as well.[63] CIITA is strongly regulated by IFN-γ, which can induce CIITA in nonlymphoid cells.[38] We show, for the first time to our knowledge, an up-regulation of CIITA in $CD8^+$ T-cell–attacked myofibers of patients with sIBM. Literature on the expression of HLA-II in sIBM is controversial. Global tissue profiling has demonstrated an increase of HLA-DP, HLA-DQ, and HLA-DR in sIBM; however, the cellular source remained uncertain.[35] Immunohistochemical studies addressing the expression of HLA-II on myofibers in inflammatory myopathies are sparse. One study[64] analyzed the expression of HLA-II in DM and PM and provided evidence that the HLA-DR expression is independent of inflammatory infiltrates. However, in sIBM, we found differential HLA-DR overexpression in $CD8^+$ T-cell–attacked myofibers (Figure 7). This discrepancy might be related to differences between the different myopathies, with IBM being dominated by $CD8^+$ T cells and DM by $CD4^+$ T cells; PM is a heterogeneous disease. The pathogenic relevance of IFN-γ–induced HLA-II expression is unknown, probably initiated by TNF-α.[65] However, (auto-) antigen presentation to $CD4^+$ T cells is unlikely because the endomysial inflammatory infiltrate in sIBM consists mainly of $CD8^+$ T cells.[7]

The IFN-γ–inducible catalytic immunoproteasome subunit PSMB8 (LMP-2) generates peptides with an increased affinity for HLA-I.[35] Previous global microarray profiling studies[35,36] showed a strong overexpression of PSMB8 in inflammatory myopathies, without revealing the cellular source. Our microarray and qPCR data attribute up-regulation of PSMB8 to A_{IBM} myofibers. This indicates an up-regulated IFN-γ signature in $A_{IBM,}$ consistent with our other findings.

It seems likely that additional IFN-γ–inducible transcripts are up-regulated in A_{IBM} myofibers. qPCR showed up-regulation of the CCL5-STAT3 system in A_{IBM} myofibers (Figure 3, L and M). CCL5, also known as RANTES, is synergistically up-regulated by TNF-α and IFN-γ[66,67] and would be expected to attract activated T cells,[39,68] thereby contributing to the local pro-inflammatory loop. Previous work[69] has shown that TNF-α up-regulates the TSP1-CD36-CD47 complex in cultured myoblasts and that the TSP1-CD36-CD47 was up-regulated in sIBM. The multifold synergies between TNF-α and IFN-γ likely play an important role in sIBM pathophysiological features. As demonstrated herein, multiple transcripts that are known to be synergistically up-regulated by TNF-α and IFN-γ, such as the CCL5-STAT3 system and IFNGR1/2, are induced on attacked myofibers. Indeed, previous studies[70,71] have suggested that the myofibers themselves are capable of producing IFN-γ–inducible chemokines that could potentially direct activated T cells. Clearly, the role of chemokines needs to be further explored in future studies.

Comparison with Other Microarray Studies in Human Inflammatory Myopathies

Previous microarray studies[35,36] in IBM, PM, DM, and degenerative muscle diseases were global and did not distinguish between muscle-derived transcripts and genes overexpressed by leukocytes present in the biopsy specimen. Determining the source of transcripts overexpressed in inflammatory myopathies is all the more important given that the ability of muscle fibers to produce certain chemokines and other proteins under inflammatory conditions has repeatedly been demonstrated.[70–72]

Regarding IBM, previously reported global microarray studies have demonstrated a strong up-regulation of HLA-I, HLA-II, PSMB8, several IFN-induced genes, and certain cytokines, such as RANTES (CCL5) and monocyte induced gamma-interferon (MIG, CXCL9) (see Supplemental Table S2 at *http://ajp.amjpathol.org*). By comparison, our study allows changes of expression patterns, in particular the overexpression of IFN-γ–inducible transcripts, to be attributed, for the first time to our knowledge, to particular subgroups of fibers. On the other hand, our data attribute the previously described Ig overexpression to tissue-invading B cells (see Supplemental Table S1 at *http://ajp.amjpathol.org*).[36,73]

Conclusion and Model

In conclusion, we found that the receptor for IFN-γ is selectively up-regulated in attacked IBM myofibers (Figure 7). This raises the crucial question of what comes first: focal inflammation or focal induction of antigen presentation and processing pathways in the attacked muscle fiber? Although we have not yet identified the initial trigger that leads to the up-regulation of HLA-I expression, we may delineate the sequence of later events.

Our findings suggest a scenario that helps explain the focal nature of the inflammatory attack in IBM muscle. First, ubiquitous HLA-I expression is induced on essentially all myofibers by unknown, possibly infectious or inflammatory, proximal triggers, thereby providing a necessary precondition for antigen recognition by $CD8^+$ T cells. Second, a $CD8^+$ T cell recognizes a surface-exposed HLA-I–bound antigen on a myofiber. This initial

encounter with antigen occurs as a random event. However, once such a contact is established, a specific immunological synapse is formed, with vectorial orientation of perforin toward the area of contact.[17] On antigen recognition and activation, the T cell starts to secrete proinflammatory cytokines and chemokines, thereby attracting and activating additional inflammatory cells, including macrophages, dendritic cells, and B cells. The cytokines produced by the inflammatory cells induce IFN-γ receptor expression on the attacked and perhaps adjacent muscle fibers, which thereby become susceptible to IFN-γ–mediated stimulation. IFN-γ–mediated signaling induces a cascade of secondary changes in the attacked fibers, increasing their susceptibility to inflammatory attack. In this way, an initial antigen recognition event by a $CD8^+$ T cell on an HLA-I–positive myofiber would be amplified, leading to strong focal inflammatory changes.

Acknowledgments

We thank Joachim Malotka and Ingrid Eiglmeier for excellent technical assistance and Drs. Dieter Jenne and Naoto Kawakami for helpful discussion of the manuscript.

References

1. Dalakas MC: Sporadic inclusion body myositis: diagnosis, pathogenesis and therapeutic strategies. Nat Clin Pract Neurol 2006, 2:437–447
2. Dalakas MC: Immunotherapy of myositis: issues, concerns and future prospects. Nat Rev Rheumatol 2010, 6:129–137
3. Griggs RC: The current status of treatment for inclusion-body myositis. Neurology 2006, 66:S30–S32
4. Wiendl H: Idiopathic inflammatory myopathies: current and future therapeutic options. Neurotherapeutics 2008, 5:548–557
5. Hilton-Jones D, Miller A, Parton M, Holton J, Sewry C, Hanna MG: Inclusion body myositis: MRC Centre for Neuromuscular Diseases, IBM workshop, London, 13 June 2008. Neuromuscul Disord 2010, 20:142–147
6. Dalakas MC: Inflammatory muscle diseases: a critical review on pathogenesis and therapies. Curr Opin Pharmacol 2010, 10:346–352
7. Engel AG, Arahata K: Monoclonal antibody analysis of mononuclear cells in myopathies, II: phenotypes of autoinvasive cells in polymyositis and inclusion body myositis. Ann Neurol 1984, 16:209–215
8. Stangel M, Mix E, Zettl UK, Gold R: Oxides and apoptosis in inflammatory myopathies. Microsc Res Tech 2001, 55:249–258
9. Dalakas MC: Inflammatory, immune, and viral aspects of inclusion-body myositis. Neurology 2006, 66:S33–S38
10. Dustin ML, Long EO: Cytotoxic immunological synapses. Immunol Rev 2010, 235:24–34
11. Lindberg C, Oldfors A, Tarkowski A: Restricted use of T cell receptor V genes in endomysial infiltrates of patients with inflammatory myopathies. Eur J Immunol 1994, 24:2659–2663
12. Amemiya K, Granger RP, Dalakas MC: Clonal restriction of T-cell receptor expression by infiltrating lymphocytes in inclusion body myositis persists over time: studies in repeated muscle biopsies. Brain 2000, 123(Pt 10):2030–2039
13. Bender A, Behrens L, Engel AG, Hohlfeld R: T-cell heterogeneity in muscle lesions of inclusion body myositis. J Neuroimmunol 1998, 84:86–91
14. Seitz S, Schneider CK, Malotka J, Nong X, Engel AG, Wekerle H, Hohlfeld R, Dornmair K: Reconstitution of paired T cell receptor alpha- and beta-chains from microdissected single cells of human inflammatory tissues. Proc Natl Acad Sci U S A 2006, 103:12057–12062
15. Hofbauer M, Wiesener S, Babbe H, Roers A, Wekerle H, Dornmair K, Hohlfeld R, Goebels N: Clonal tracking of autoaggressive T cells in polymyositis by combining laser microdissection, single-cell PCR, and CDR3-spectratype analysis. Proc Natl Acad Sci U S A 2003, 100:4090–4095
16. Dimitri D, Benveniste O, Dubourg O, Maisonobe T, Eymard B, Amoura Z, Jean L, Tiev K, Piette JC, Klatzmann D, Herson S, Boyer O: Shared blood and muscle CD8+ T-cell expansions in inclusion body myositis. Brain 2006, 129:986–995
17. Goebels N, Michaelis D, Engelhardt M, Huber S, Bender A, Pongratz D, Johnson MA, Wekerle H, Tschopp J, Jenne D, Hohlfeld R: Differential expression of perforin in muscle-infiltrating T cells in polymyositis and dermatomyositis. J Clin Invest 1996, 97:2905–2910
18. Hohlfeld R, Engel AG: Lysis of myotubes by alloreactive cytotoxic T cells and natural killer cells: relevance to myoblast transplantation. J Clin Invest 1990, 86:370–374
19. Hohlfeld R, Engel AG: Coculture with autologous myotubes of cytotoxic T cells isolated from muscle in inflammatory myopathies. Ann Neurol 1991, 29:498–507
20. McDouall RM, Dunn MJ, Dubowitz V: Expression of class I and class II MHC antigens in neuromuscular diseases. J Neurol Sci 1989, 89:213–226
21. Karpati G, Pouliot Y, Carpenter S: Expression of immunoreactive major histocompatibility complex products in human skeletal muscles. Ann Neurol 1988, 23:64–72
22. Bartoccioni E, Gallucci S, Scuderi F, Ricci E, Servidei S, Broccolini A, Tonali P: MHC class I, MHC class II and intercellular adhesion molecule-1 (ICAM-1) expression in inflammatory myopathies. Clin Exp Immunol 1994, 95:166–172
23. Jain A, Sharma MC, Sarkar C, Bhatia R, Singh S, Handa R: Major histocompatibility complex class I and II detection as a diagnostic tool in idiopathic inflammatory myopathies. Arch Pathol Lab Med 2007, 131:1070–1076
24. Emslie-Smith AM, Arahata K, Engel AG: Major histocompatibility complex class I antigen expression, immunolocalization of interferon subtypes, and T cell-mediated cytotoxicity in myopathies. Hum Pathol 1989, 20:224–231
25. Arahata K, Engel AG: Monoclonal antibody analysis of mononuclear cells in myopathies, I: quantitation of subsets according to diagnosis and sites of accumulation and demonstration and counts of muscle fibers invaded by T cells. Ann Neurol 1984, 16:193–208
26. Chahin N, Engel AG: Correlation of muscle biopsy, clinical course, and outcome in PM and sporadic IBM. Neurology 2008, 70:418–424
27. Lynoe N, Sandlund M, Dahlqvist G, Jacobsson L: Informed consent: study of quality of information given to participants in a clinical trial. BMJ 1991, 303:610–613
28. Dalakas MC: Clinical, immunopathologic, and therapeutic considerations of inflammatory myopathies. Clin Neuropharmacol 1992, 15:327–351
29. Junker A, Ivanidze J, Malotka J, Eiglmeier I, Lassmann H, Wekerle H, Meinl E, Hohlfeld R, Dornmair K: Multiple sclerosis: T-cell receptor expression in distinct brain regions. Brain 2007, 130:2789–2799
30. Storey JD, Tibshirani R: Statistical methods for identifying differentially expressed genes in DNA microarrays. Methods Mol Biol 2003, 224:149–157
31. Schmittgen TD, Livak KJ: Analyzing real-time PCR data by the comparative C(T) method. Nat Protoc 2008, 3:1101–1108
32. Livak KJ, Schmittgen TD: Analysis of relative gene expression data using real-time quantitative PCR and the 2(-Delta Delta C(T)) Method. Methods 2001, 25:402–408
33. Wang Y, Liu D, Chen P, Koeffler HP, Tong X, Xie D: Negative feedback regulation of IFN-gamma pathway by IFN regulatory factor 2 in esophageal cancers. Cancer Res 2008, 68:1136–1143
34. Butticè G, Miller J, Wang L, Smith BD: Interferon-gamma induces major histocompatibility class II transactivator (CIITA), which mediates collagen repression and major histocompatibility class II activation by human aortic smooth muscle cells. Circ Res 2006, 98:472–479
35. Greenberg SA, Sanoudou D, Haslett JN, Kohane IS, Kunkel LM, Beggs AH, Amato AA: Molecular profiles of inflammatory myopathies. Neurology 2002, 59:1170–1182
36. Greenberg SA, Bradshaw EM, Pinkus JL, Pinkus GS, Burleson T, Due B, Bregoli L, O'Connor KC, Amato AA: Plasma cells in muscle in inclusion body myositis and polymyositis. Neurology 2005, 65:1782–1787
37. Kloetzel PM: Antigen processing by the proteasome. Nat Rev Mol Cell Biol 2001, 2:179–187

38. van den Elsen PJ, Holling TM, Kuipers HF, Van der Stoep N: Transcriptional regulation of antigen presentation. Curr Opin Immunol 2004, 16:67–75
39. Kovacic JC, Gupta R, Lee AC, Ma M, Fang F, Tolbert CN, Walts AD, Beltran LE, San H, Chen G, St Hilaire C, Boehm M: Stat3-dependent acute Rantes production in vascular smooth muscle cells modulates inflammation following arterial injury in mice. J Clin Invest 2010, 120:303–314
40. Larkin J III, Johnson HM, Subramaniam PS: Differential nuclear localization of the IFNGR-1 and IFNGR-2 subunits of the IFN-gamma receptor complex following activation by IFN-gamma. J Interferon Cytokine Res 2000, 20:565–576
41. van der Pas J, Hengstman GJ, ter Laak HJ, Borm GF, van Engelen BG: Diagnostic value of MHC class I staining in idiopathic inflammatory myopathies. J Neurol Neurosurg Psychiatry 2004, 75:136–139
42. Wiendl H, Behrens L, Maier S, Johnson MA, Weiss EH, Hohlfeld R: Muscle fibers in inflammatory myopathies and cultured myoblasts express the nonclassical major histocompatibility antigen HLA-G. Ann Neurol 2000, 48:679–684
43. Tezak Z, Hoffman EP, Lutz JL, Fedczyna TO, Stephan D, Bremer EG, Krasnoselska-Riz I, Kumar A, Pachman LM: Gene expression profiling in DQA1*0501+ children with untreated dermatomyositis: a novel model of pathogenesis. J Immunol 2002, 168:4154–4163
44. Feldman BM, Rider LG, Reed AM, Pachman LM: Juvenile dermatomyositis and other idiopathic inflammatory myopathies of childhood. Lancet 2008, 371:2201–2212
45. Grundtman C, Bruton J, Yamada T, Ostberg T, Pisetsky DS, Harris HE, Andersson U, Lundberg IE, Westerblad H: Effects of HMGB1 on in vitro responses of isolated muscle fibers and functional aspects in skeletal muscles of idiopathic inflammatory myopathies. FASEB J 2010, 24:570–578
46. Illa I, Nath A, Dalakas M: Immunocytochemical and virological characteristics of HIV-associated inflammatory myopathies: similarities with seronegative polymyositis. Ann Neurol 1991, 29:474–481
47. Leon-Monzon M, Illa I, Dalakas MC: Polymyositis in patients infected with human T-cell leukemia virus type I: the role of the virus in the cause of the disease. Ann Neurol 1994, 36:643–649
48. Cupler EJ, Leon-Monzon M, Miller J, Semino-Mora C, Anderson TL, Dalakas MC: Inclusion body myositis in HIV-1 and HTLV-1 infected patients. Brain 1996, 119(Pt 6):1887–1893
49. Bao S, King NJ, Dos Remedios CG: Flavivirus induces MHC antigen on human myoblasts: a model of autoimmune myositis? Muscle Nerve 1992, 15:1271–1277
50. Askanas V, Engel WK: Sporadic inclusion-body myositis: a proposed key pathogenetic role of the abnormalities of the ubiquitin-proteasome system, and protein misfolding and aggregation. Acta Myol 2005, 24:17–24
51. Askanas V, Engel WK: Inclusion-body myositis: muscle-fiber molecular pathology and possible pathogenic significance of its similarity to Alzheimer's and Parkinson's disease brains. Acta Neuropathol 2008, 116:583–595
52. Vattemi G, Nogalska A, King EW, D'Agostino C, Checler F, Askanas V: Amyloid-beta42 is preferentially accumulated in muscle fibers of patients with sporadic inclusion-body myositis. Acta Neuropathol 2009, 117:569–574
53. Karpati G, O'Ferrall EK: Sporadic inclusion body myositis: pathogenic considerations. Ann Neurol 2009, 65:7–11
54. Schmidt J, Barthel K, Wrede A, Salajegheh M, Bahr M, Dalakas MC: Interrelation of inflammation and APP in sIBM: iL-1 beta induces accumulation of beta-amyloid in skeletal muscle. Brain 2008, 131:1228–1240
55. Banwell BL, Engel AG: AlphaB-crystallin immunolocalization yields new insights into inclusion body myositis. Neurology 2000, 54:1033–1041
56. Nagaraju K, Raben N, Loeffler L, Parker T, Rochon PJ, Lee E, Danning C, Wada R, Thompson C, Bahtiyar G, Craft J, Hooft Van HR, Plotz P: Conditional up-regulation of MHC class I in skeletal muscle leads to self-sustaining autoimmune myositis and myositis-specific autoantibodies. Proc Natl Acad Sci U S A 2000, 97:9209–9214
57. Nagaraju K, Casciola-Rosen L, Lundberg I, Rawat R, Cutting S, Thapliyal R, Chang J, Dwivedi S, Mitsak M, Chen YW, Plotz P, Rosen A, Hoffman E, Raben N: Activation of the endoplasmic reticulum stress response in autoimmune myositis: potential role in muscle fiber damage and dysfunction. Arthritis Rheum 2005, 52:1824–1835
58. Li CK, Knopp P, Moncrieffe H, Singh B, Shah S, Nagaraju K, Varsani H, Gao B, Wedderburn LR: Overexpression of MHC class I heavy chain protein in young skeletal muscle leads to severe myositis: implications for juvenile myositis. Am J Pathol 2009, 175:1030–1040
59. Hohlfeld R, Engel AG: HLA expression in myoblasts. Neurology 1991, 41:2015
60. Ahmed CM, Johnson HM: IFN-gamma and its receptor subunit IFNGR1 are recruited to the IFN-gamma-activated sequence element at the promoter site of IFN-gamma-activated genes: evidence of transactivational activity in IFNGR1. J Immunol 2006, 177:315–321
61. Illa I, Gallardo E, Gimeno R, Serrano C, Ferrer I, Juarez C: Signal transducer and activator of transcription 1 in human muscle: implications in inflammatory myopathies. Am J Pathol 1997, 151:81–88
62. Leibundgut-Landmann S, Waldburger JM, Krawczyk M, Otten LA, Suter T, Fontana A, Acha-Orbea H, Reith W: Mini-review: specificity and expression of CIITA, the master regulator of MHC class II genes. Eur J Immunol 2004, 34:1513–1525
63. Gobin SJ, Peijnenburg A, van Eggermond M, van Zutphen M, van den Berg R, van den Elsen PJ: The RFX complex is crucial for the constitutive and CIITA-mediated transactivation of MHC class I and beta2-microglobulin genes. Immunity 1998, 9:531–541
64. Englund P, Lindroos E, Nennesmo I, Klareskog L, Lundberg IE: Skeletal muscle fibers express major histocompatibility complex class II antigens independently of inflammatory infiltrates in inflammatory myopathies. Am J Pathol 2001, 159:1263–1273
65. Keller CW, Fokken C, Turville SG, Lünemann A, Schmidt J, Münz C, Lunemann JD: TNF-alpha induces macroautophagy and regulates MHC class II expression in human skeletal muscle cells. J Biol Chem 2011, 286:3970–3980
66. Lee AH, Hong JH, Seo YS: Tumour necrosis factor-alpha and interferon-gamma synergistically activate the RANTES promoter through nuclear factor kappaB and interferon regulatory factor 1 (IRF-1) transcription factors. Biochem J 2000, 350(Pt 1):131–138
67. Hiroi M, Ohmori Y: The transcriptional coactivator CREB-binding protein cooperates with STAT1 and NF-kappa B for synergistic transcriptional activation of the CXC ligand 9/monokine induced by interferon-gamma gene. J Biol Chem 2003, 278:651–660
68. Flier J, Boorsma DM, van Beek PJ, Nieboer C, Stoof TJ, Willemze R, Tensen CP: Differential expression of CXCR3 targeting chemokines CXCL10, CXCL9, and CXCL11 in different types of skin inflammation. J Pathol 2001, 194:398–405
69. Salajegheh M, Raju R, Schmidt J, Dalakas MC: Upregulation of thrombospondin-1(TSP-1) and its binding partners, CD36 and CD47, in sporadic inclusion body myositis. J Neuroimmunol 2007, 187:166–174
70. Raju R, Vasconcelos O, Granger R, Dalakas MC: Expression of IFN-gamma-inducible chemokines in inclusion body myositis. J Neuroimmunol 2003, 141:125–131
71. Tateyama M, Fujihara K, Misu T, Itoyama Y: CCR7+ myeloid dendritic cells together with CCR7+ T cells and CCR7+ macrophages invade CCL19+ nonnecrotic muscle fibers in inclusion body myositis. J Neurol Sci 2009, 279:47–52
72. Hohlfeld R, Goebels N, Engel AG: Cellular mechanisms in inflammatory myopathies. Baillieres Clin Neurol 1993, 2:617–635
73. Bradshaw EM, Orihuela A, McArdel SL, Salajegheh M, Amato AA, Hafler DA, Greenberg SA, O'Connor KC: A local antigen-driven humoral response is present in the inflammatory myopathies. J Immunol 2007, 178:547–556